Supporting Information

Facile Chemical Synthesis of High-Performance Pt/C Catalyst in Specialized Morphology

Jie Yang[a †], *Rurong Liu*[a †], *Chenyang Shen*[a †], *Xiaoxia Hou*[a], *Chenjia Liang*[a], *Ruiyao Zhao*[a], *Chao Yue*[a], *Yingxuan Zhao*[a], *Qing Liu*[a], *Ningze Gao*[a], *Liwen Wang*[a], *Tao Wang*[b], *Wenhua Hou*[a]*, *Weiping Ding*[a]*

[a] *Key Lab of Mesoscopic Chemistry, School of Chemistry and Chemical Engineering, Nanjing University, Nanjing 210023, China*

[b] *Jiangsu Meso Catalytic Materials Technology Co., Ltd, Science and Technology Innovation Park, 36 Huada Road, Zhangjiagang Free Trade Zone, Jiangsu 215634, China*

[†] *These authors contributed equally to this work.*

[*] Corresponding authors. E-mail address: dingwp@nju.edu.cn; whou@nju.edu.cn

Experimental section

Synthesis of ssPt and Pt/C

Urea modified carbon was prepared using traditional impregnation method. Typically, 0.08 g urea was dissolved into 5 ml deionized water at room temperature and added to 1 g XC-72 with continuously stirring, then the mixture stands for 24 h and dried overnight in an 80 ^{o}C oven and after thoroughly grounded, the urea modified carbon was obtained.

ssPt and Pt/C were prepared using the same ethylene glycol reduction (EGR) method with different support. Typically, 0.08 g support was added to 25 ml ethylene glycol first, then 25 ml 0.004 mol/L $H_2PtCl_6 \cdot 6H_2O$ was added dropwise, the mixture was heated to 120 ^{o}C for 12 h, after filtration, washing and drying, the targeted sample is prepared.

Structure and electrochemical characterization

The specific surface area and pore size distribution were acquired by N_2 adsorption-desorption isotherms at 77 K performed on Micromeritics ASAP2460. The morphology and structure of the catalyst were observed by HRTEM (Talos F200S G2). XRD patterns were collected on a Phillips X'pert Pro diffractometer with Cu Kα radiation at 40 kV and 40 mA. XPS was performed on Thermo

Fisher ESCALAB 250Xi, all dates have been adjusted by carbon.

H_2-O_2 titration: the 10 mg catalyst was pretreated at Ar atmosphere for 1 h at 80 °C, after cooling to room temperature, O_2 was switched and kept flowing for 0.5 h for adsorption, then the sample was cooled to -78 °C in dry ice and Ar was switched in again to remove the physically adsorbed O_2, after another 0.5 h flowing, the Ar was switched to 5 vol% H_2/Ar, and the sample was than heated to room temperature. A mass spectrometer monitored the signal of H_2 throughout.

H_2/D_2 exchange: 10 mg catalyst was pretreated at 5 vol% H_2/Ar, atmosphere for 1 h at 80 °C, then cooled to -78 °C, subsequently Ar was switched to remove the physically adsorbed H_2, next 5 vol% D_2/Ar was introduced for the H-D exchange from -78 °C to room temperature, with a mass spectrometer monitoring the H-D signal.

O_2/air switching of cathode fluent: the MEAs were prepared using 0.1 mg/cm^2 Pt of ssPt or Pt/C, respectively. The anode catalysts were all JM Pt/C catalyst in loading of 0.1 mg/cm^2 Pt, unless otherwise specified. During the test, the fuel cells were firstly operated at a current density of 10 mA/cm^2 under steady state with cathode oxygen fluent of 50 mL/min. Then the oxygen fluent was switched to air and the variation of current with time was recorded.

Electrochemical test

The electrochemical tests were conducted using a three-electrode system on an electrochemical workstation (CHI 760e). The working electrode was prepared by ultrasonically dispersing 5 mg catalyst in 1975 μl isopropanol and 25 μl Nafion (5 wt%). After 45 minutes of ultrasonication, 10 μl of the ink was transferred onto a 5 mm diameter glassy carbon electrode and dried at room temperature. Graphite and Hg/Hg_2Cl_2 electrode were served as counter and reference electrodes in 0.1 M $HClO_4$ solution. Cyclic voltammetry (CV) was conducted at the potential of 0.05-1.2 V (vs. RHE) with a scan rate of 20 mV/s in N_2-saturated 0.1 M $HClO_4$ solution. The rotating disk electrode (RDE) method was used to test ORR activity in O_2-saturated 0.1 M $HClO_4$ solution at the potential of 0.05-1.2 V (vs. RHE) with 20 mV/s scan rate and 1600 r/min rotation rate. The accelerated durability tests (ADTs) were performed by applying the cyclic voltammetry between 0.6 and 0.9 V (vs. RHE) with a scan rate of 500 mV/s for 50,000 cycles.

Membrane electrode assembly

The catalyst ink was prepared by mixing the catalyst with water, Nafion solution, and isopropanol in a weight ratio of 1:3:3:20. Then ultrasonicated for two hours. After that it was ultrasonically spayed onto Nafion membrane (Gore proton exchange membrane M765.08 8 μm). The cathodic catalyst layer loading for ssPt and commercial 40 wt % JM Pt/C was set at 0.1 mg/cm^2 Pt, while commercial JM 40% Pt/C with a 0.1 mg/cm^2 Pt loading was used as anode. A single cell unit was assembled with the catalyst-coated membrane (CCM) sandwiched between two gas diffusion layers. The performance of the single cell was tested by a fuel cell station with an effective area of 1 cm^2. The I-V curve was measured at cell temperature of 80 ^{o}C with 200 ml/min H_2 flow rate, 200 ml/min O_2 flow rate and 100% relative humidity.

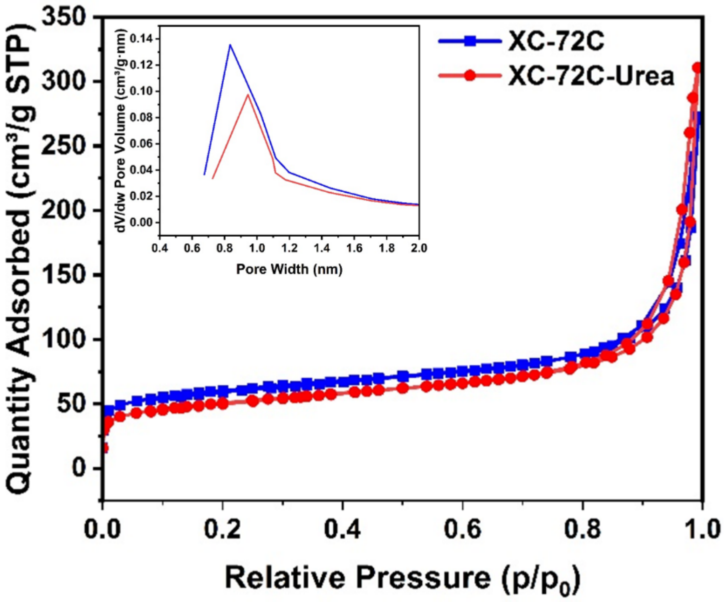

Figure S1. N_2 sorption isotherm and pore size distribution of XC-72C-urea and XC-72C

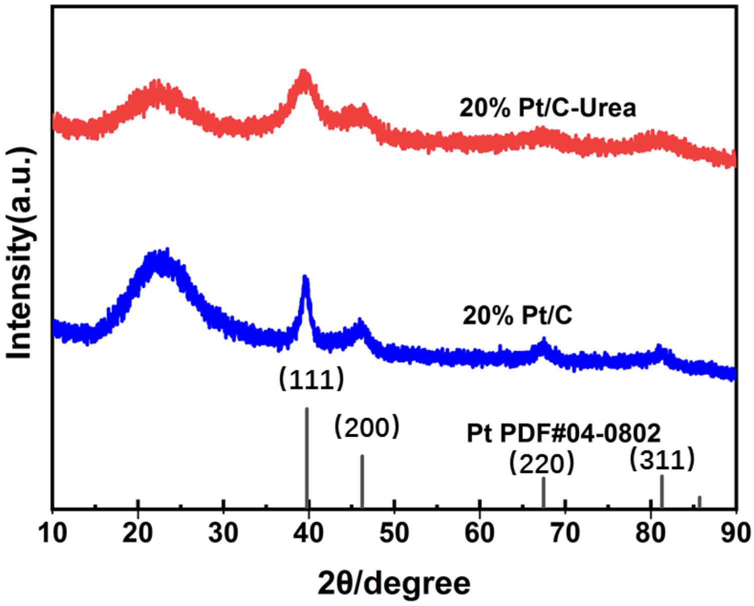

Figure S2. XRD patterns of ssPt and Pt/C

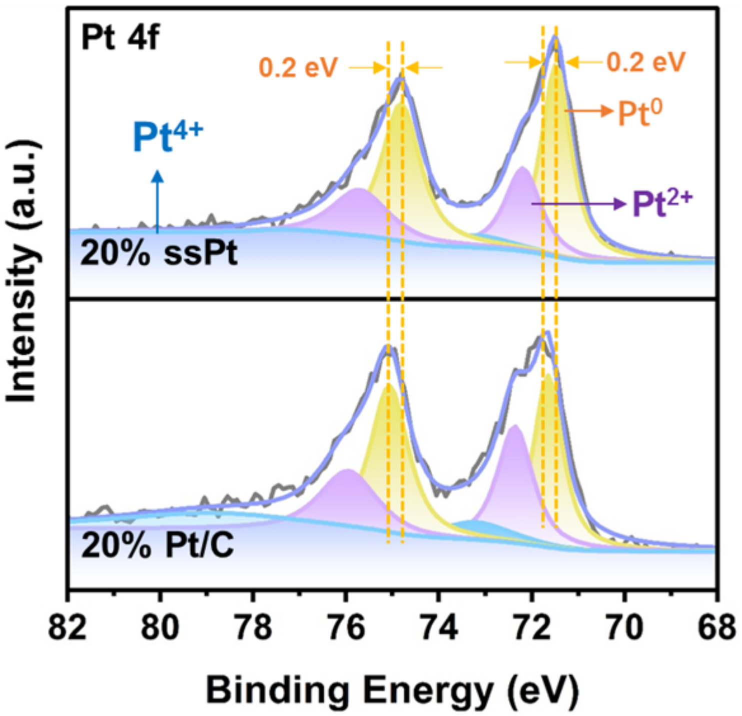

Fig. S3. Results of XPS measurements on catalysts of ssPt and Pt/C

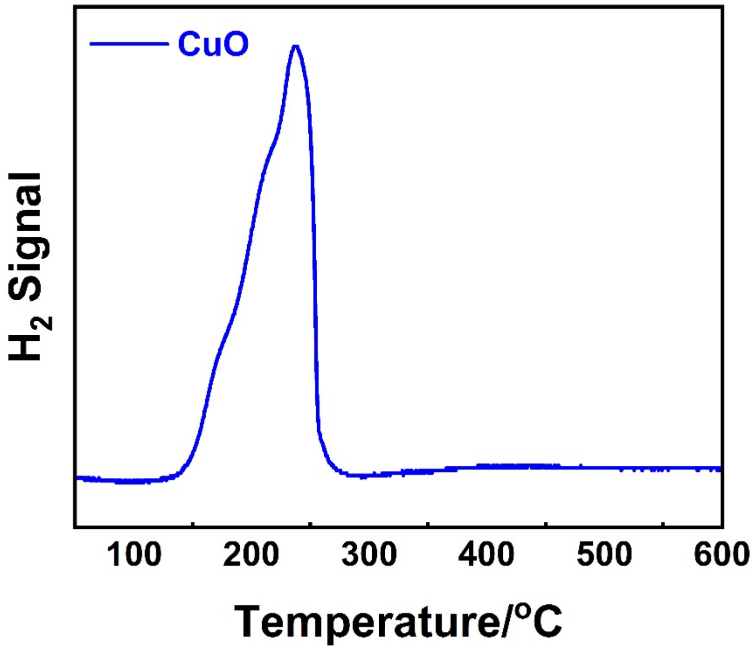

Figure S4. H_2-TPR result of CuO as standard for quantity analysis.

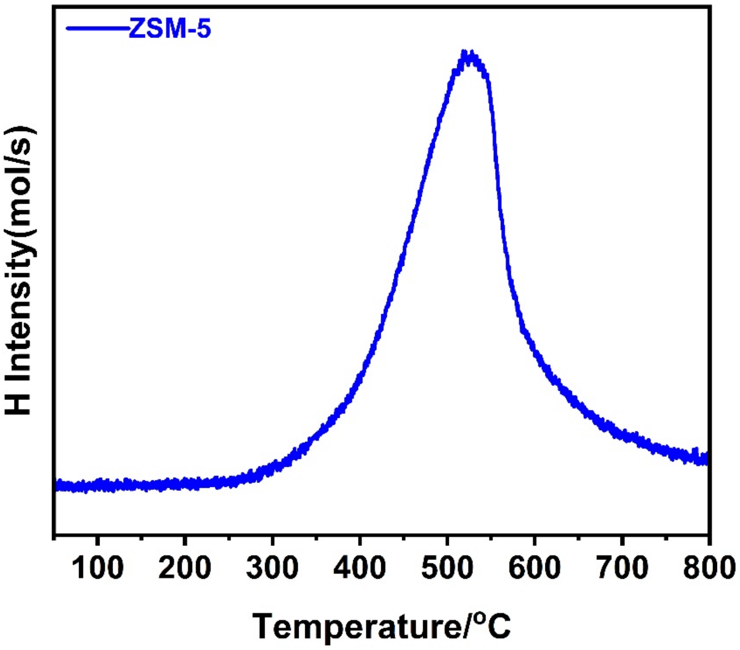

Figure S5. H_2/D_2 exchange of HZSM-5 zeolite as standard for calibration.

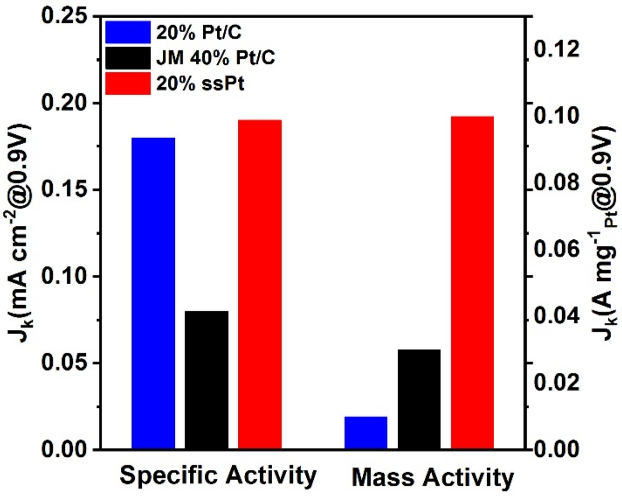

Figure S6. Specific activity and mass activity of the Pt/C, JM Pt/C and ssPt

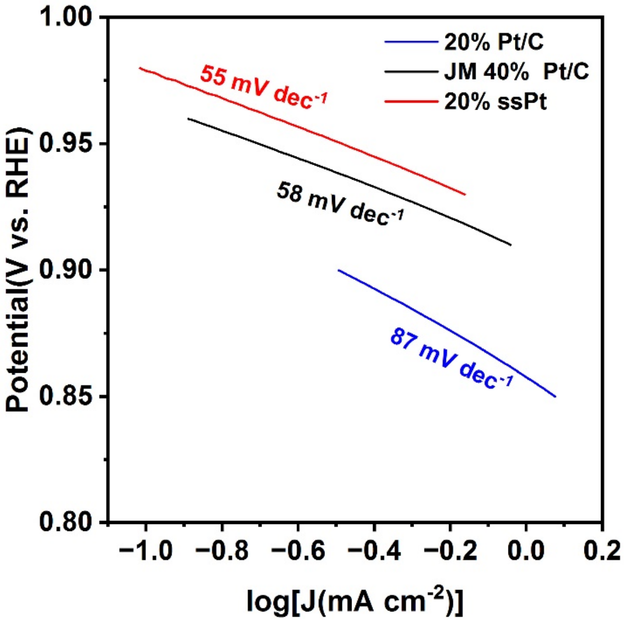

Figure S7. Tafel slope of the Pt/C, JM Pt/C and ssPt

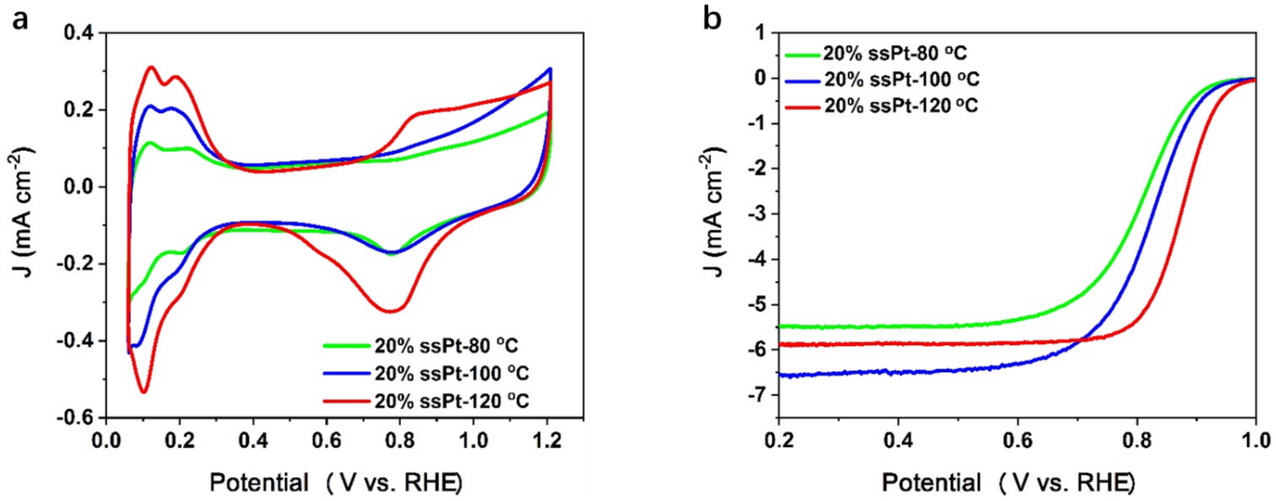

Figure S8. CV(a) and LSV(b) results of the ssPt synthesized at different temperatures.

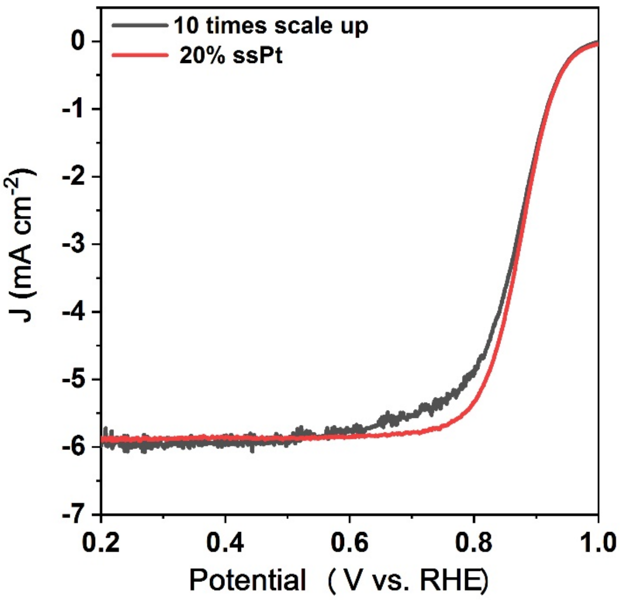

Figure S9 the LSV curves from the 10 times scale up

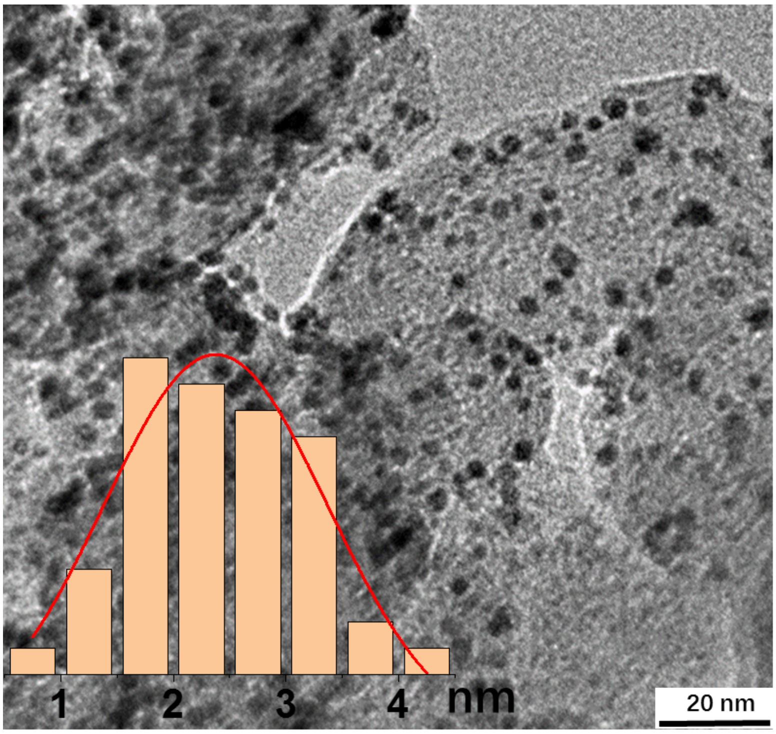

Figure S10. TEM image of ssPt (20wt.% Pt) after 50K cycles of ADT test.

Table S1. Catalyst compositions analyzed by ICP.

Catalyst	Pt/C	ssPt
Pt content (wt.%)	15.6	19.3

Table S2. The valences of Pt measured by XPS.

Catalyst	Pt^0	Pt^{2+}	Pt^{4+}
20% Pt/C	47%	39%	14%
ssPt	60%	31%	9%

Table S3. The exchangeable hydrogen on the surface of catalysts measured by H_2/D_2 exchange.

Catalyst	Peak 1[*1]	Peak 2[*2]	Peak 3[*3]
Pt/C (20wt.% Pt)	0.16	1.60	2.33
ssPt (20wt.% Pt)	0.33	3.15	3.01

[*1] The ratio of hydrogen adsorbed on Pt to total number of Pt atom; [*2] The ratio of hydrogen adsorbed on the carbon near Pt particle to total number of Pt atom; [*3] The ratio of hydrogen chemically bonded to the carbon support to total number of Pt atom.

Table S4. ECSA of different catalysts

Catalyst	Pt/C	JM Pt/C	ssPt	ssPt after ADT
ECSA(m^2/g)	7	37	50	49

Table S5. The comparison of half cell performance between ssPt and reported catalysts in literature

Catalysts	Electrolyte	Half-wave potential	Ref.
Pt/C_{-N}	0.1 M $HClO_4$	0.85	1
Pt_1Co_{100}/N-GCNT	0.1 M $HClO_4$	0.85	2
$Pt_3(C_{12}N_6O_6)_2$MOF	0.5 M H_2SO_4	0.84	3
Pt@C/C700	0.1 M $HClO_4$	0.88	4
Pt@Mn-SAs/N-C	0.1 M $HClO_4$	0.89	5
Pt/C@NC	0.1 M $HClO_4$	0.84	6
Pt/C-TiO_2	0.1 M $HClO_4$	0.86	7
Pt/S-C-1	0.1 M $HClO_4$	0.87	8
ssPt	0.1 M $HClO_4$	0.87	This work

Table S6. Synthetics conditions of ethylene glycol reduction for Pt/C catalysts

Catalyst	Temperature/^{o}C	Adjustment of pH	Ref.
Pt/C	140	NaOH	9
Pt/C	160	NaOH	10
Pt/C	140	Na_3Cit	11
Pt/C	160	NaOH	12
$Pt/CeO_2\text{-}TiO_2$	160	NaOH	13
Pt/CeO_2	150	-	14
Pt/CeO_2	130	NaOH	15
Pt/TiO_2	170	-	16
Pt/TiO_2(Ov)-C	140	-	17
ssPt	120	-	This work

Table S7. ECSA of ssPt synthesized at different temperatures.

Synthesis Temp. (^{o}C)	80	100	120
ECSA (m^2/g)	10	25	50

Table S8. The comparison of MEA performance between ssPt and reported catalysts in literature

Cathode Catalysts	Pt Content (mg/cm^2)	Back pressure (bar)	Cell temperature(^{o}C)	Peak Power density (W/cm^2)	Ref.
DC-Pt_1Co_1/CNT	0.035	0.5	80	1.26	18
PtMg/C-31	0.08	0.5	80	1.57	19
PtCo30Ni10@NG	0.1	1.5	80	2.03	20
Pt_FG	0.2	2.0	70	1.29	21
pCN@NHCS-Fe/Pt	0.1	1.0	80	0.96	22
$L1_0$-PtCoIn@Pt	0.1	2.5	80	1.99	23
Pt/CNT	0.1	0	80	1.31	24
TiO_2/Pt/C	0.4	-	70	1.03	25
PtNiCo/NC	0.12	0.15	70	1.07	26
ssPt	0.1	0	80	1.57	This work

Reference

[1] Z. Xiang, W. Li, F. Liu , *Electrochem. Commun*., **2021**, 127, 107039.

[2] X. Cheng, Y. Wang, Y. Lu, *Appl. Catal. B*, **2022**, 306, 121112.

[3] R. Iqbal, S. Ali, A. Saleem, *Chem. Eng. J.* , **2023**, 455, 140799.

[4] Y. Jiang, Y. Wang, J. Qian, *Int. J. Hydrogen Energy*, **2024**, 51, 578-586.

[5] L. Gong, J. Zhu, F. Xia, *ACS Catal.* , **2023**, 13, 4012-4020.

[6] D. Liu, J. Zhang, D. Liu, *J. Phys. Chem. Lett.*, **2022**, 13, 2019-2026.

[7] Y. Liu, J. Ye, F. Kong, *Catalysts,* **2022**, 12.

[8] Y. Xie, Z. Wang, M. Xu, *ChemSusChem*, **2024**, 17, e202301819.

[9] R. Zeng, K. Wang, W. Shao, *Chin. J. Catal.* , **2020,** 41, 820-829.

[10] Y.-J. Wang, N. Zhao, B. Fang, *RSC Advances*, **2015,** 5, 56570-56577.

[11] F. Wu, Y. Liu, C. Wu, *J. Mater. Sci. Technol*, **2010**, 26, 705-710

[12] J. Quinson, M. Inaba, S. Neumann, *ACS Catal.* , **2018,** 8, 6627-6635.

[13] Y. Shi, J. Wang, R. Zhou, *Chemosphere*, **2021,** 265, 129127.

[14] C.M.S. Queiroz, A.P. Machado, A.R.N. Paiva, *Materials for Renewable and Sustainable Energy*, **2019,** 8-17.

[15] X. Tang, B. Zhang, Y. Li, Catal. Let. , **2004**, 97, 163-169

[16] L. Lei, Q. Cao, J. Ma, *Molecules*, **2024,** 29, 1450.

[17] Z. Wang, X. Jin, F. Chen, X. Kuang, *J Colloid Interface Sci*, **2023,** 650, 901-912.

[18] L. Tian, X. Gao, M. Zhu, *Adv. Mater.*, **2025**, e2417095.

[19] C. Gyan-Barimah, J.S.P. Mantha, H.Y. Lee, *Nat. Commun.,* **2024**, 15, 7034.

[20] L. Sun, Y. Yin, B. Ren, Nano Energy, **2024**, 120, 109154.

[21] M.S. Garapati, E. de Prado, V. Vretenar, *ACS Appl Mater Interfaces*, **2025**, .

[22] Y. Wang, G. Tan, Q. Yi, *ACS Appl. Energy Mater.* , **2023**, 6, 1228-1238.

[23] L. Zhao, Z. Zhu, J. Wang, Angew Chem Int Ed Engl, **2025**, e202501805.

[24] Y. Pei, W. Zhu, R. Yue, *J. Mater. Chem. A*, **2024**, 12, 739-747.

[25] W.-J. Lee, S. Bera, H. Woo, *Chem. Mater.* , 2022, 34, 5949-5959.

[26] S. Hanif, X. Shi, N. Iqbal, *Appl. Catal. B*, 2019, 258, 117947